Research Square

Preprints are preliminary reports that have not undergone peer review.
They should not be considered conclusive, used to inform clinical practice,
or referenced by the media as validated information.

Comparison of Dioxin and Heavy Metal and Other Pollutants Emission Characteristics from Domestic Solid Waste Gasifiers in Typical Arid and Humid Regions

Zitong Liu

zitongliu00@163.com

Research Institute of Solid Waste Management, Chinese Research Academy of Environmental Sciences, Beijing, China and College of Environmental Science and Engineering, Nanjing Tech University, Nanjing, China https://orcid.org/0009-0005-5542-1237

Chao Chen

Research Institute of Solid Waste Management, Chinese Research Academy of Environmental Sciences, Beijing, China

Li Li

Research Institute of Solid Waste Management, Chinese Research Academy of Environmental Sciences, Beijing, China

Lei Wang

College of Environmental Science and Engineering, Nanjing Tech University, Nanjing, China

Dahai Yan

Research Institute of Solid Waste Management, Chinese Research Academy of Environmental Sciences, Beijing, China https://orcid.org/0000-0001-5079-0707

Research Article

Keywords: Rural domestic waste, Gasification and incineration, Pollutant emission characteristics, Dioxin, HSC thermodynamic simulation

Posted Date: November 3rd, 2026

DOI: https://doi.org/10.21203/rs.3.rs-10637172/v1

License: This work is licensed under a Creative Commons Attribution 4.0 International License.
Read Full License

Comparison of Dioxin and Heavy Metal and Other Pollutants Emission Characteristics from Domestic Solid Waste Gasifiers in Typical Arid and Humid Regions

Zitong Liu[a,b], Chao Chen[a], Li Li[a], Lei Wang[b], Dahai Yan[a,*]

[a] Research Institute of Solid Waste Management, Chinese Research Academy of Environmental Sciences, Beijing 100012, China

[b] College of Environmental Science and Engineering, Nanjing Tech University, Nanjing 211816, China

Funding: This work was supported by the National Key Research and Development Program of China (grant number 2024YFC3909005, 2024YFC3810303)

Abstract: This study compares the emission characteristics of heavy metals, dioxins, and other pollutants from two small-scale gasification incinerators treating rural domestic waste in different regions of China. The results showed that Facility A exceeded the emission limits for NO_x and total hydrocarbons (THC) in the flue gas, with maximum concentrations of 698 and 521 mg/Nm^3, respectively, and significant fluctuations were observed during the monitoring period. The concentrations of heavy metals in the flue gas of Facility A were generally higher than those in Facility B, with Zn reaching a maximum of 449 μg/Nm^3. On the first monitoring day at Facility B, the flue gas Tl concentration was 83.6 μg/Nm^3, but it decreased rapidly over the following two days. Dioxin emission levels in the flue gas from both facilities were relatively low, ranging from 0.023 to 0.0512 ng TEQ/m^3. In Facility A, 2,3,4,7,8-PeCDF accounted for the highest proportion (17.84%) of all dioxin congeners in the flue gas. The concentrations of Zn, Ba, and Mn were generally high in both the slag and fly ash of Facility A. Dioxins showed significant enrichment in the fly ash of Facility A, with the highest concentration reaching 26,833 ng TEQ/kg, far exceeding regulatory standards. Among the fly ash congeners, 2,3,4,7,8-PeCDF was the most predominant, accounting for 20.31%. Finally, thermodynamic equilibrium simulations for NO_x and incomplete combustion gases were performed using HSC Chemistry software. Comparison with measured values confirmed that the operating conditions of the secondary combustion chamber are strongly correlated with the generation of NO_x and unburned gases. These results confirm that such small-scale facilities have developed considerably in recent years, and technologies capable of controlling environmental risks at a lower level have already emerged.

Keywords: Rural domestic waste; Gasification and incineration; Pollutant emission characteristics; Dioxin; HSC thermodynamic simulation

First author: Zitong Liu

e-mail: zitongliu00@163.com

Corresponding author:

Dahai Yan

e-mail: seavsland@163.com

Introduction

Urban domestic waste treatment facilities and their pollution emission control systems are relatively well-developed; therefore, greater attention should be paid to rural areas in terms of environmental protection and regional environmental quality. In most rural and township areas of China, per capita daily waste generation ranges from 0.7 to 1.1 kg/(person·day), resulting in approximately 200 million tons of solid waste annually and posing serious environmental pollution issues (Arista et al. 2023). In rural areas, domestic waste generation is highly decentralized, and the cost of waste collection and transport in mountainous regions is relatively high (Teng and Zhou 2023). Moreover, the amount of waste generated is insufficient to support the continuous and stable operation of large-scale incineration facilities with a processing capacity exceeding 400 t/d.

Small-scale heat treatment technology for domestic waste has become one of the solutions to this problem. Such facilities occupy a small footprint and achieve effective volume reduction. There are three main types of small-scale heat treatment processes for municipal solid waste: incineration, pyrolysis, and gasification. Gasification technology converts waste into high-temperature flue gas, combustible gas, and ash under an oxygen-deficient environment, using air and steam as gasifying agents (Cheng et al. 2025). It offers advantages such as good operational stability and lower pollution risk, and is therefore currently used more frequently. The processing scale of small facilities can be roughly divided into two categories: facilities with a scale of 100-200 t/d are mostly used for county-level municipal solid waste treatment, while those with a capacity of ≤100 t/d are mainly used for the treatment of municipal solid waste in towns and villages. Currently, many villages and towns in China use small-scale heat treatment equipment with a processing capacity of around 10 t/d. Previous research has identified many issues with small-scale municipal solid waste heat treatment facilities, particularly in meeting pollution risk control standards. Li Xiaoyuan et al. (Li et al. 2024) found that the emission factors of dioxins in the flue gas and fly ash of seven small-scale high-temperature treatment facilities were 0.34-288.37 and 0.16-289.75 μg I-TEQ/t, respectively. Currently, there is very little relevant research abroad, and small-scale waste heat treatment facilities are primarily used as supplements to large waste incinerators and large landfills. Only a few studies in China have investigated the pollution emissions of small-scale municipal solid waste heat treatment facilities to some extent. Wen Teng et al. (Teng et al. 2024) used air-staged gasification and incineration technology to process the combustible components of rural domestic waste, comparing the effects of incineration and gasification-incineration on the migration of heavy metals. The results showed that gasification-incineration can effectively reduce the volatility of heavy metals, with the volatility of Cu being reduced by as much as 12.99%. Li Jian et al. (Li et al. 2024) studied the

emissions of pollutants (NO_x and SO_2) from rural solid waste (RSW), established a self-sustaining pyrolysis model for RSW, proposed the direct combustion of pyrolysis gas and pyrolysis oil as the driving force for pyrolysis, and suggested using pyrolysis char to prepare carbon-based materials. It was found that compared with direct combustion, NO_x and SO_2 emissions during pyrolytic combustion were reduced by 86% and 100%, respectively. This proves that pyrolytic combustion is a feasible method for treating RSW, as it not only has low operational costs (no additional energy input) but also minimizes pollutant emissions. Lei Ming et al. (Lei et al. 2019) used the AERMOD model and a respiratory exposure assessment method to conduct an environmental risk assessment of PCDD/F emissions from three small-scale municipal solid waste incinerators in Southwest China. The results showed that PCDD/F emission concentrations in the flue gas reached 4.88-24.88 ng TEQ/m^3, far higher than the emission requirement of <0.1 ng TEQ/m^3. Yang Lili et al. (Yang et al. 2019) conducted a preliminary investigation of dioxins (PCDD/Fs) and polychlorinated naphthalenes (PCNs) emitted from a small-scale waste incineration furnace. They found that the concentration and toxicity equivalent of PCDD/Fs were 153 ng/m^3 and 5.6 ng TEQ/m^3, respectively, far exceeding the limits for municipal solid waste incinerators in China. Polychlorinated dibenzo-p-dioxins and polychlorinated dibenzofurans (PCDD/Fs), also known as dioxins, are highly toxic tricyclic aromatic organic compounds, with the most toxic substance being 2,3,7,8-TCDD (Zhao et al. 2022). Currently, three known synthesis pathways for dioxins exist: high-temperature gas-phase synthesis, precursor synthesis, and de novo synthesis (Peng et al. 2016).

In summary, there is currently a lack of investigation and research on small-scale waste treatment facilities in rural and township areas. These small facilities have significant room for improvement in terms of technical equipment levels, emission risks of characteristic pollutants, economic costs, and the resource utilization of fly ash and slag. This study conducted field research on two small-scale municipal solid waste heat treatment facilities in rural areas of China. By exploring the daily operation conditions, pollutant emission characteristics, and making horizontal comparisons between the two facilities, it was found that in terms of overall operational stability and flue gas treatment effectiveness, both facilities generally met the requirements.

1 Materials and methods

1.1 Research subjects

The two facilities covered by this study are located in Chifeng, Inner Mongolia, and Lincang, Yunnan, respectively. The basic details of the two facilities are shown (Table 1).

Table 1. Small-scale heat treatment facilities for domestic waste used in experiments

Furnace type	Facility number	Location	Scale(t/d)
Gasification incinerator	A	Chifeng, Inner Mongolia	15

1.2 Materials

The samples covered by this study include domestic waste, flue gas, fly ash and furnace slag.

1.2.1 Sampling of domestic waste

Sampling was conducted according to the Chinese standard "Sampling and Analysis Methods for Domestic Waste" (CJ/T 313-2009). Sampling bags were used following the quartering method, and the waste was stirred to ensure uniform mixing before sampling. Facility A provided three pretreated waste samples, while Facility B provided one sample.

1.2.2 Sampling of flue gas

The flue gas sampling locations for Facilities A and B were both at the chimney, with a chimney height of 15 m. The average flue gas temperatures at the sampling points were 57.4 and 54.8 ℃, respectively. The standard dry flue gas flow rates were 1,110.9 and 1,041.2 m^3/h, and the oxygen contents were measured. The monitoring work lasted for three days, with two flue gas samples collected each day, and the average values of the daily tests were analyzed.

Sampling of conventional pollutants in flue gas was conducted according to "The determination of particulates and sampling methods of gaseous pollutants from exhaust gas of stationary source" (GB/T 16157-1996). SO_2, NO_x, CO, THC, and PM were collected using an automatic flue gas analyzer (ZR-3260, Junray, China). Each sample, except for THC, was collected for 30 minutes, while HCl and HF were collected using a dual-channel flue gas sampler (ZR-3710, Junray, China) for one hour each.

Heavy metal sampling was conducted according to "Ambient air and stationary source emission-Determination of metals in ambient particulate matter-Inductively coupled plasma/mass spectrometry (ICP-MS)" (HJ 657-2013). Samples were collected using an automatic smoke and gas comprehensive tester (ZR-3260, Junray, China), with a sampling duration of one hour per sample, and 30 minutes for Hg.

Dioxin sampling followed "Ambient air and waste gas Determination of polychlorinated dibenzo-p-dioxins (PCDDs) and polychlorinated dibenzofurans (PCDFs) Isotope dilution HRGC-HRMS" (HJ 77.2-2008) and used a waste gas dioxin sampler (ZR-3720, Junray, China) for isokinetic sampling. An internal standard was added before sampling, and the sampling duration was two hours.

1.2.3 Sampling of fly ash

The fly ash sampling point at Facility A was located at the baghouse dust collector. Three samples were collected daily using sampling bags according to the simple random sampling method set out in "Technical specifications on sampling and sample preparation from industry solid waste" (HJ/T 20-1998). To ensure that the flue gas and bottom ash

samples were taken from the same batch of municipal solid waste fed into the furnace, fly ash sampling at Facility A was carried out six hours after flue gas sampling began. The collected fly ash was granular, with a relatively fine particle size and a pale grey colour. Facility B employed a wet dust removal process; after capture, the fly ash formed a sludge-like substance that fell into a recirculation tank and was periodically pumped back to the gasifier for treatment via a sludge pump. Consequently, it was not possible to collect fly ash samples from Facility B.

1.2.4 Sampling of slag

Slag samples were taken from the slag layer at the bottom of the gasifier. Three samples were collected daily using sampling bags according to the simple random sampling method specified in HJ/T 20-1998. To ensure that the flue gas and slag samples were taken from the same batch of municipal solid waste fed into the furnace, slag sampling at Facility A was carried out six hours after the start of flue gas sampling, while at Facility B it was carried out 48 hours after the start of flue gas sampling. The slag at Facility A was greyish-brown, with some ash and slag fused together, resulting in larger particles, indicating severe coking within the furnace. The slag at Facility B was light grey and had a smaller particle size.

1.3 Methods

1.3.1 The physical composition, moisture content, calorific value, elemental analysis, content of harmful elements and heavy metal content of domestic waste

The physical composition and moisture content of the waste were determined according to the methods set out in CJ/T 313-2009, using an electronic balance (ML204/02, METTLER TOLEDO, SUI) and an electric hot-air forced-circulation oven (DHG-9013A, JBS, China). The lower heating value was determined according to "Determination of calorific value of coal" (GB/T 213-2008) using a microcomputer-controlled fully automatic calorimeter (ZDHW-600, Hua Yuan Instrument and Meters, China). Elemental analysis was conducted according to "General detecting methods for the chemical characteristic of domestic refuse" (CJ/T 96-2013) using an organic elemental analyzer (vario EL, Elementar Analysensysteme GmbH, DEU). The F, Cl and S contents in the waste were determined according to "Solid waste-Determination of fluoride-Alkali fusion-ion selective electrode method" (HJ 999-2018), "Characterization of waste-Halogen and sulfur content - Oxygen combustion in closed systems and determination methods" (EN 14582:2016), and "Determination of total sulfur in coal" (GB/T 214-2007). An ion analyzer (PXSJ-227L, Lei-ci, China) was used to determine F content, while a calorimeter (ZDHW-600, Hua Yuan Instrument and Meters, China) and an ion chromatograph (CIC-D120, SHINE, China) were used to determine Cl content. A fully automatic sulfur analyzer (5E-8S/AII, CKIC, China) was used for S content. Heavy metal concentrations were determined according to "Solid waste-Determination of 22 metal elements-Inductively coupled plasma optical emission spectrometry" (HJ 781-2016), using an

inductively coupled plasma emission spectrometer (iCAP 7200 DUO, Thermo Fisher, USA). Mercury was determined using an atomic fluorescence spectrometer (AFS-2202E, HAIGUANG INSTRUMENT, China) according to "Solid Waste-Determination of Mercury, Arsenic, Selenium, Bismuth, Antimony-Microwave Dissolution/Atomic Fluorescence Spectrometry" (HJ 702-2014).

1.3.2 Conventional pollutants

The detection of conventional pollutants in flue gas (SO_2, NO_x, HCl, HF, THC, CO and PM) was carried out according to the following methods: SO_2 and NO_x were analyzed using an automatic integrated flue gas analyzer (ZR-3260, Junray, China). HF and HCl were analyzed using an ion chromatograph (CIC-D120, SHINE, China) according to "Ambient air and stationary source emissions-Determination of Hydrogen Chloride-Ion Chromatography" (HJ 549-2016) and "Stationary source emission-Determination of hydrogen fluoride-Ion chromatography" (HJ 688-2019). THC was analyzed using a gas chromatograph (GC9790II, FULI INSTRUMENTS, China) according to "Stationary source emission-Determination of total hydrocarbons, methane and nonmethane hydrocarbons-Gas chromatography" (HJ 38-2017). CO was analyzed using an automatic smoke and flue gas analyzer (ZR-3260, Junray, China) according to "Stationary source emission-Determination of carbon monoxid-Fixed potential by electrolysis method" (HJ 973-2018). PM was analyzed according to "Stationary source emission-Determination of mass concentration of particulate matter at low concentration-Manual gravimetric method" (HJ 836-2017), using an electronic balance (ESJ30-5B, TUO XI ELECTRONIC, China).

1.3.3 Heavy metals

The determination of heavy metal concentrations in flue gas was carried out according to "Ambient air and stationary source emission-Determination of metals in ambient particulate matter-Inductively coupled plasma/mass spectrometry (ICP-MS)" (HJ 657-2013). During analysis, the filter membrane was cut into small pieces, added to a mixture of nitric and hydrochloric acids for digestion, and then analyzed using an inductively coupled plasma mass spectrometer (ICAP RQ, Thermo Fisher, USA). Mercury (Hg) content was determined according to "Stationary source emission-Determination of mercury-Cold atomic absorption spectrophotometry" (HJ 543-2009) using a cold atom absorption spectrophotometer (F732-VJ, JU CHUANG ENVIRONMENTAL, China).

The heavy metal content in slag and fly ash was determined according to "Solid waste-Determination of 22 metal elements-Inductively coupled plasma optical emission spectrometry" (HJ 781-2016), using an inductively coupled plasma emission spectrometer (iCAP 7200 DUO, Thermo Fisher, USA). Mercury content was determined according to "Solid Waste-Determination of Mercury, Arsenic, Selenium, Bismuth, Antimony-Microwave Dissolution/Atomic Fluorescence Spectrometry" (HJ 702-2014), using an atomic fluorescence spectrometer (AFS-2202E, HAIGUANG INSTRUMENT, China).

1.3.4 Dioxin

Dioxins in flue gas were determined using the method specified in HJ 77.2-2008. After sample collection, the samples were first subjected to Soxhlet extraction with toluene as the solvent for 24 hours. The sample solution was concentrated to 1 mL using a concentrator, and the concentrated solution was quantitatively transferred to a silica gel column for purification; the eluate was then concentrated to 1 mL. Subsequently, the eluate was dried under high-purity nitrogen to remove excess solvent and concentrated to a slightly moist state. Finally, an internal standard was added, the solution was made up to the appropriate volume with toluene, transferred to a sample vial as the final analytical sample,

and analyzed for dioxin concentration using a high-resolution gas chromatography-high-resolution mass spectrometry (HRGC-HRMS) system (Thermo Fisher, DFS, USA). The spiked recovery rates ranged from 76% to 112%, meeting quality control requirements.

For the determination of dioxins in fly ash, according to the method specified in "Solid waste Determination of polychlorinated dibenzo-p-dioxins (PCDDs) and polychlorinated dibenzofurans (PCDFs) Isotope dilution HRGC-HRMS" (HJ 77.3-2008), an internal standard was added prior to sample preparation. A specified quantity of the prepared solid sample was weighed and treated with hydrochloric acid for one hour, stirring the sample until no further foaming occurred. The hydrochloric acid treatment solution was filtered using a Büchner funnel, and the sample was thoroughly rinsed with water, followed by removal of moisture with a small amount of acetone. The filter membrane and sample were placed in a petri dish and transferred to a clean desiccator for thorough drying. A known quantity of dichloromethane was added to the hydrochloric acid treatment solution, and the mixture was shaken to extract the compounds; this process was repeated three times. The extract was then dehydrated using anhydrous sodium sulphate. The thoroughly dried filter membrane and sample were subjected to Soxhlet extraction using toluene as the solvent. The resulting extract and the toluene extract were combined to form the sample solution. Subsequent processing steps were identical to those for gaseous samples: after purification, concentration and the addition of an internal standard, the sample was analyzed using a high-resolution double-focusing magnetron-induced electron-beam ionization mass spectrometer (Trace 1310 DFS IE-3867, Thermo Scientific, USA).

The amount of dioxins entering the slag is extremely small compared with that in fly ash. Previous studies indicated that in typical municipal waste incinerators, the dioxin content in fly ash was 319 ng/g, with a toxicity equivalent of 6.7 ng I-TEQ/g, whereas in slag, these values were 38.7 pg/g and 1.1 pg I-TEQ/g (Table 2) (Yang et al. 2024). Given the 10,000-fold difference between the two fractions, this contribution can be disregarded; therefore, no determination of dioxins in the slag will be carried out here.

Table 2. Concentration of dioxins in the fly ash and slag from the waste incinerator

Matter	Mass concentration (pg/g)	TEQ (pg I-TEQ/g)
Fly ash	319,000	6,700
Slag	38.7	1.1

1.3.5 HSC thermodynamic simulation

This study utilized the "Equilibrium Composition" module in HSC Chemistry 6.0 software to simulate the products formed during the heat treatment process. The elemental composition of the system was configured via "Create New Input File (Give Elements)", the reactants were selected and their quantities set, and the simulation conditions were defined. Following this, the "Calculate Equilibrium Composition" button was clicked to perform the thermodynamic equilibrium calculation, yielding the composition of each substance when the system reaches equilibrium under theoretical conditions (Jeon et al. 2012; Wang 2023).

2 Results and discussion

2.1 The basic information of domestic waste

2.1.1 Climate types and elements of the national economy

The Chifeng region of Inner Mongolia, where Facility A is located, is generally arid throughout the year and

experiences strong winds and sandstorms (Zhao et al. 2026). With an average annual humidity of 48.8% and an average annual precipitation of just 381 mm, it has a temperate semi-arid continental monsoon climate. In contrast, Lincang in Yunnan, where Facility B is situated, is relatively humid with abundant rainfall. It has an average annual humidity of 75.8% and an average annual precipitation of 1,259 mm, and is characterized by a subtropical low-latitude plateau mountainous monsoon climate. This is one of the reasons for the significant difference in the moisture content and calorific value of municipal solid waste between the two regions.

The key economic indicators for the two locations are shown (Table 3). It can be seen that although Lincang's population is only half that of Chifeng, rural areas account for 60.73% of its total population, whereas in Chifeng, rural areas account for 43.32% of the total population; thus, the proportion of the rural population in Chifeng is relatively smaller than that in Lincang. Compared with Beijing, where the rural population accounts for only 11.84%, both locations exhibit a high proportion of rural residents, indicating a significant demand for the treatment and disposal of rural domestic waste. Furthermore, Chifeng's GDP is twice that of Lincang. Chifeng's primary industry is manufacturing (Zhao et al. 2023), whereas Lincang's is agriculture. This leads to regional differences in the physical composition of domestic waste between the two cities: at Facility A, the waste entering the incinerator consists mainly of rubber and plastic materials, whereas at Facility B, it consists primarily of paper, rubber and plastic materials, and food waste-a composition similar to that of urban domestic waste (Du et al. 2021).

Table 3. Elements of the national economy

Place	Total population (ten thousand people)	Rural population (ten thousand people)	GDP (hundred million yuan)	GDP per capita (yuan)
Chifeng, Inner Mongolia	393.1	170.3	2,322.1	58,787
Lincang, Yunnan	219.5	133.3	1,150.19	52,317

2.1.2 The basic nature of domestic waste

Municipal solid waste in both locations is collected as a mixed stream and is not sorted prior to collection and transport.

In the rural areas of Chifeng, Inner Mongolia (Facility A), domestic waste contains a high proportion of non-combustible materials, primarily rubber and plastics (62.17%) and textiles (9.79%). It is also mixed with considerable amounts of agricultural and forestry waste, such as dry grass and straw (20.20%). The remaining categories, including food waste, glass, and paper, account for less than 10% of the total (Table 4). Because food waste is likely used mainly

as fertilizer for home-grown crops or as livestock feed, its moisture content is extremely low, and its lower heating value is high (4,926 kJ/kg). This is one of the reasons for slag coking under excessively high furnace temperatures (Jia et al. 2024; Yuan et al. 2025). The elemental composition of the waste entering the furnace is dominated by C (47.43%) and H (19.92%) (Fig. 1). Compared with rural waste in Lincang, the C and H contents are higher, indicating a greater proportion of combustible components, which is the primary reason for the higher calorific value. Facility A processes waste with a higher Cl content than Facility B, reflecting its higher proportion of rubber and plastic waste (Kots et al. 2023), while the F and S contents are comparable.

Facility B is located in Lincang, Yunnan, and its municipal waste composition is relatively comprehensive, consisting mainly of paper (31.93%), rubber and plastic materials (26.14%), and food waste (including agricultural and forestry waste, 20.44%). As the waste is fed into the furnace without prior composting (Table 4), it has a high moisture content, resulting in a relatively low calorific value of 3,048 kJ/kg. It is generally accepted that the lower heating value of waste treated by incineration should not be less than 3,300 kJ/kg; however, this facility generally meets the requirements. Among the waste entering the furnace, carbon (C) has the highest content at 37.88% (Fig. 1). This corresponds to the high proportions of paper, rubber and plastic, and food waste (Li et al. 2024), reflecting the characteristic that organic matter dominates the municipal solid waste being processed.

Table 4. Basic properties of the rural domestic waste fed into the furnace

Facilities	Elemental analysis (%)				Harmful elements analysis (mg/kg)			Moisture Content (%)	lower calorific value (kJ/kg)
	C	H	O	N	F	Cl	S		
A	47.43	6.07	19.92	1.11	193	3,304	1,440	13.56	4,926
B	37.88	8.804	6.432	0.439	170	1,360	1,059	40.87	3,048

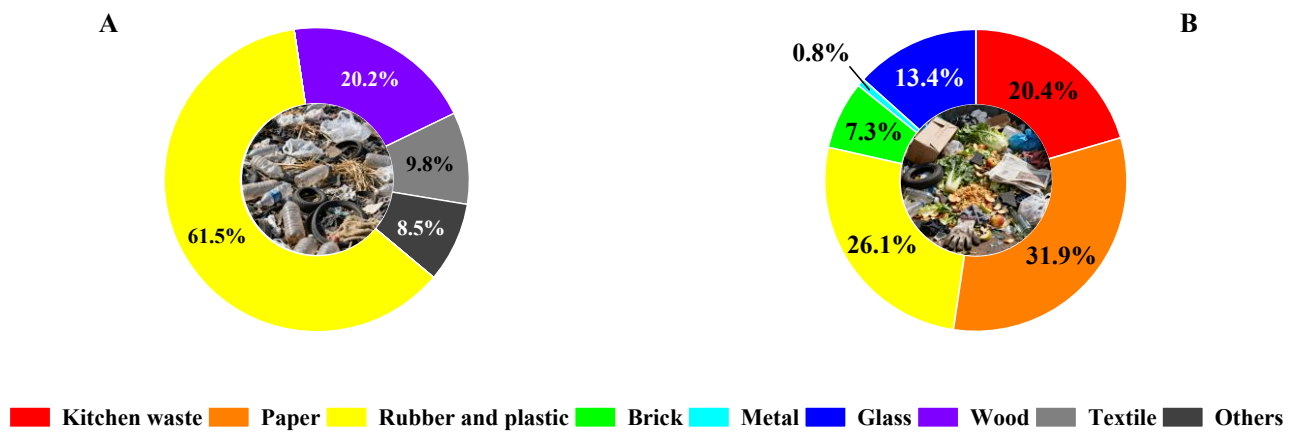


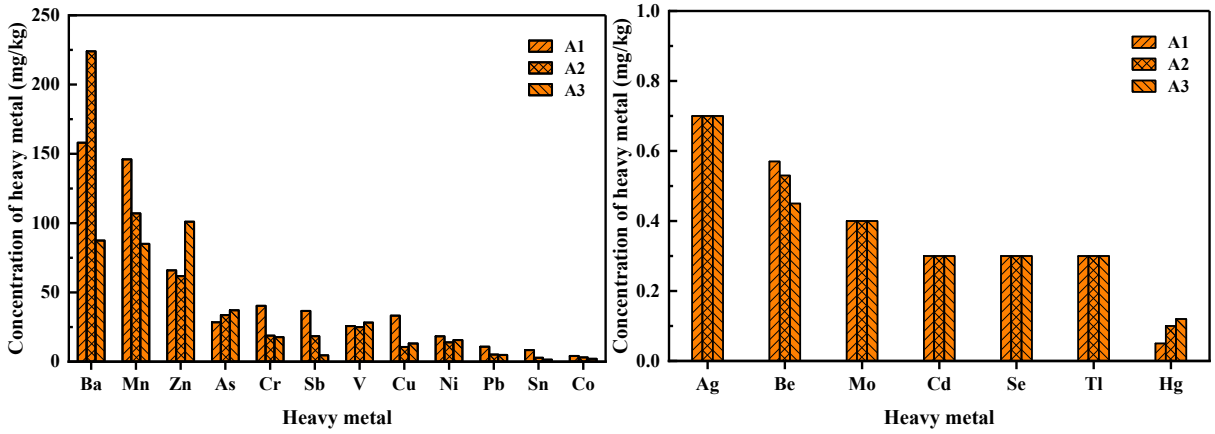
Fig. 1. Physical composition of rural domestic waste

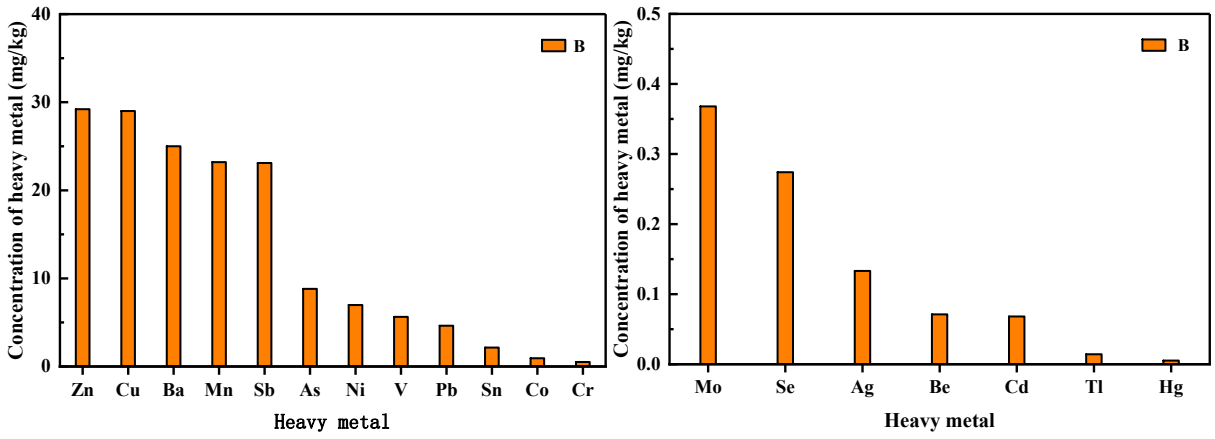
2.1.3 The content of heavy metals in domestic waste

The concentrations of metallic elements in the municipal solid waste samples are shown below. A1, A2, A3, B1, B2 and B3 represent samples collected on the first, second and third days of the three-day monitoring period at Facilities A and B, respectively; the same applies below.

The results indicate that the overall heavy metal content in municipal solid waste is relatively low (Fig. 2). For waste entering the incinerator at Facility A, Ba, Mn and Zn are the metal elements with the highest concentrations, while Ag, Mo, Cd, Se, Tl and Hg were largely not detected. The concentration of Ba reached 224 mg/kg in sample A2; the high proportion of rubber and plastic waste in the waste stream is likely the primary cause of this phenomenon. $BaSO_4$, characterized by its high density, chemical inertness, isometric particle shape and high filling capacity (Lan 2010), is widely used in the production of rubber and plastic products, with the amount of $BaSO_4$ varying across different rubber products. In plastic products, $BaSO_4$ enhances corrosion resistance, heat resistance and strength, while also improving the product's appearance (Turner and Filella 2020); it is used in materials such as PP, ABS and PET. Meanwhile, the concentrations of Mn and Zn reached 112.8 mg/kg and 76.2 mg/kg, respectively.

In contrast, the heavy metal concentrations in the waste fed into Facility B were generally low; even the highest concentration of Zn was only 29.2 mg/kg. This phenomenon is attributed to the significant differences in the composition of municipal solid waste between the two sites. The rubber, plastic and paper materials in the waste fed into Facility A contributed substantial amounts of heavy metals (Jia et al. 2015), resulting in relatively higher levels of certain heavy metal elements compared with Facility B. No detectable levels of Ag, Mo, Cd, Se and Tl were found in the waste from Facility A, nor were any detectable levels of Cr and Hg found in the waste from Facility B.



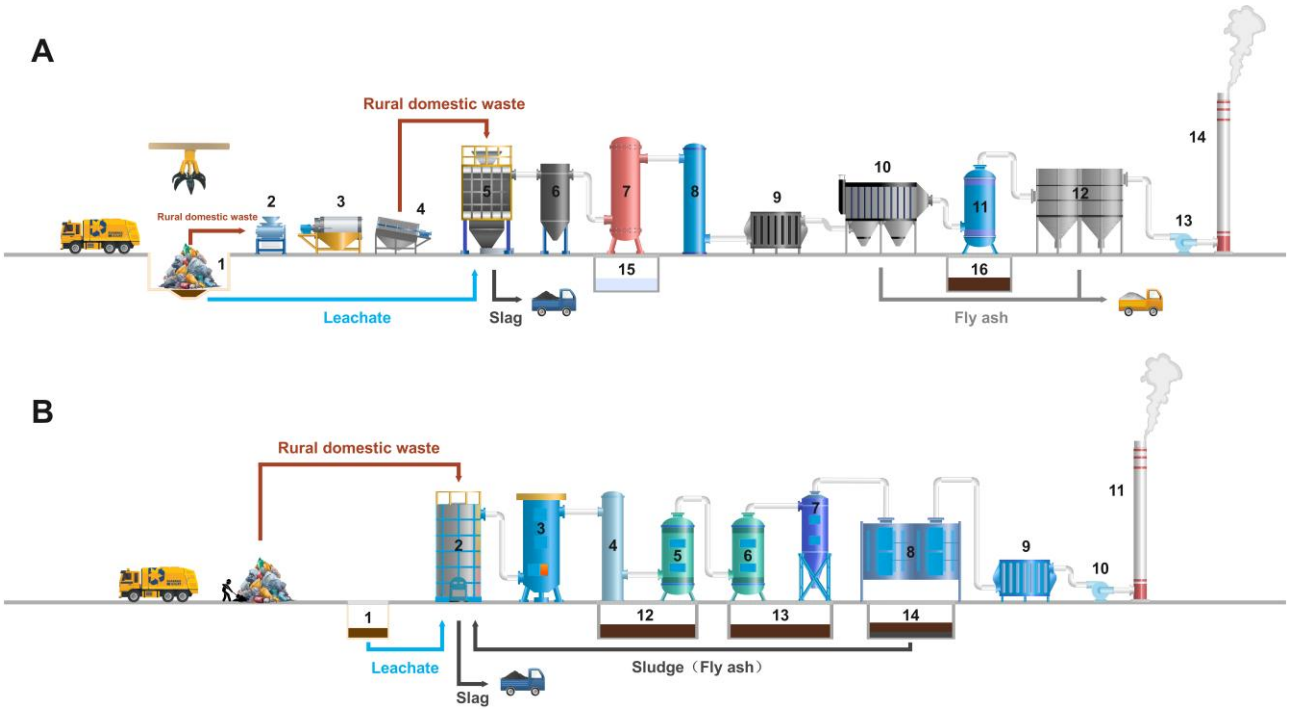


Note: When the content is below the detection limit, it is plotted as half the detection limit.

Fig. 2. Content of heavy metals in rural domestic waste

2.2 Process comparison

The process flows for Facilities A and B differ in several respects, including the pre-treatment system, the design of the gasifier and the flue gas cleaning process (Fig. 3 and Table 5).



Notes: A: 1. Waste storage pit; 2. Crusher; 3. Magnetic separator; 4. Drum screening machine; 5. Gasifier; 6. Secondary combustion chamber; 7. Heat exchanger; 8. Rapid cooling tower; 9. Activated carbon injection device; 10. Fabric filter; 11. Wet deacidification tower; 12. Electrostatic precipitator; 13. Induced draft fan; 14. Chimney;

15. Circulating water pool ①; 16. Circulating water pool ②

B: 1. Leachate collection tank; 2. Gasifier; 3. Secondary combustion chamber; 4. Rapid cooling tower; 5. High-pressure spray tower; 6. Wet deacidification tower; 7. Liquid-gas separation tower; 8. Wet electrostatic precipitator; 9. Activated carbon injection device; 10. Induced draft fan; 11. Chimney.; 12. Circulating water pool ①; 13. Circulating water pool

②; 14. Circulating water pool ③

Fig. 3. Comparison of process flows

Table 5. Differences in technical processes

Facilities	Pretreatment system	High-temperature treatment system	Flue gas treatment system
A	waste storage pit+Crusher+ Magnetic separator+ Drum screening machine	The flue gas doesn't pass through the garbage layer	Two-stage dust removal facilities
B	Simple manual sorting	The flue gas passes through the garbage layer	Single-stage dust removal facilities

2.2.1 Preprocessing system

The most significant difference between the two facilities in terms of technical processes lies in the pre-treatment stage.

At Facility A, construction and demolition waste accounts for nearly 50% of the municipal solid waste entering the furnace; therefore, after the waste enters the storage pit, it must undergo crushing, magnetic separation and screening before being fed into the furnace. This optimizes the efficiency of the subsequent gasification and incineration stages and separates recyclable materials from the waste.

Facility B does not have a waste storage pit, and the waste undergoes only simple manual sorting prior to feeding. However, the requirements and configuration of the pre-treatment system are closely linked to the facility's geographical location and the composition of the municipal solid waste. Facility A's feedstock contains a significant amount of inorganic non-combustible material; without a certain degree of pre-treatment, it is difficult to meet the calorific value requirements for the feedstock. In contrast, Facility B's feedstock composition is relatively standard, allowing it to be fed into the system for processing without the need for extensive pre-treatment.

2.2.2 Gasifier

There are certain differences in the structural design of the gasifiers at the two facilities (Fig. 4).

At Facility A, the flue gas does not pass through the waste bed but enters the internal secondary combustion chamber of the gasifier via a bypass side inlet before proceeding to the external secondary combustion chamber; thus, the waste bed does not act to trap pollutants. At Facility B, however, the flue gas flows counter-currently through the waste bed before entering the secondary combustion chamber. Some of the heavy metals and dioxins released from the waste in the high-temperature gasification bed are intercepted and solidified in the fly ash and furnace slag during their ascent with the flue gas, due to condensation by the overlying waste or adsorption onto fine particulate matter. Consequently, the concentration of pollutants ultimately entering the flue gas is reduced.

Monitoring revealed that in Facility A, the gasification rate of domestic waste in the primary combustion chamber was excessively rapid, resulting in poor combustion efficiency and causing the bed to collapse. The process from feed to slag discharge took only 6-8 hours; this may also explain the high heat loss rate of slag in Facility A, which reached a maximum of 4.2%. In contrast, the process from feed to slag discharge in Facility B took approximately 48 hours, with municipal solid waste remaining in the pyrolysis gasifier for over 48 hours. Consequently, the heat loss rate of the slag at Facility B was only 1.2% at most, demonstrating that the slag contained minimal residual unburned organic matter. This indicates that the waste was thoroughly combusted, with effective heat treatment ensuring the complete decomposition, gasification and combustion of organic matter.

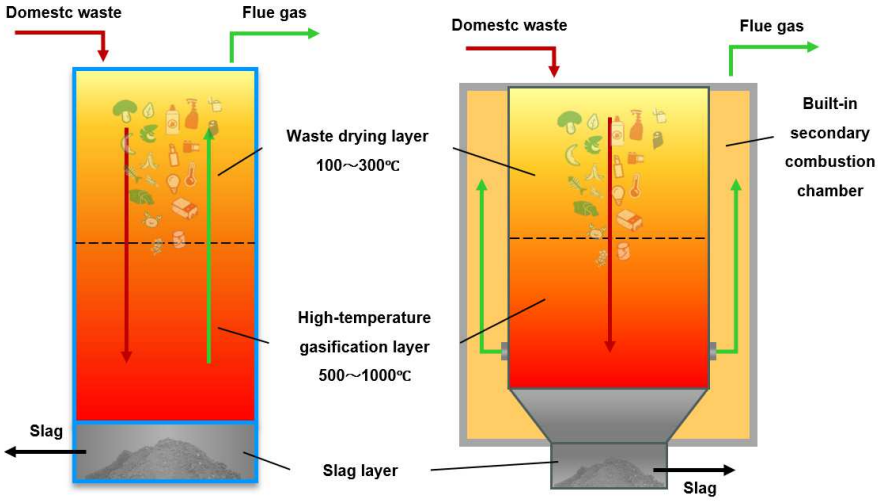
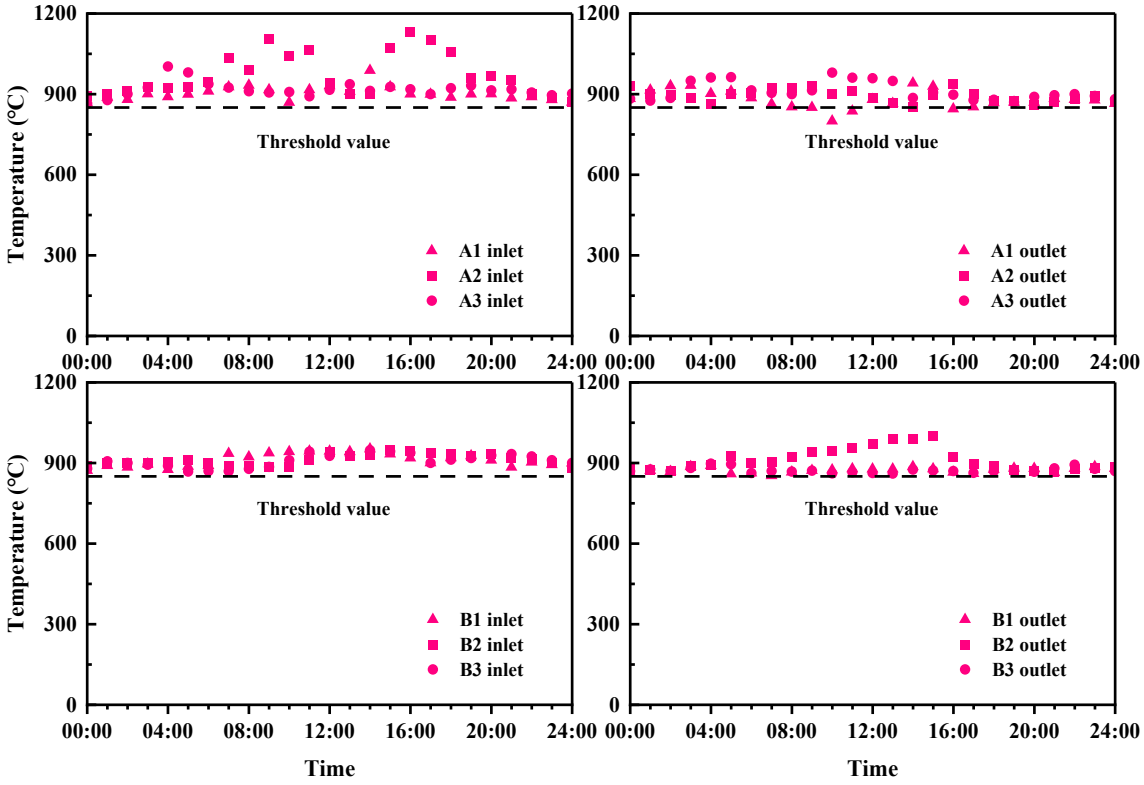


Fig. 4. Comparison of gasifiers

Facilities A and B were monitored during different seasons; Facility A was monitored during the summer, while Facility B was monitored during the autumn. There were slight differences between the two facilities in terms of combustion stability in the secondary combustion chamber. Variations in the 24-hour temperature profile of the secondary combustion chamber during the monitoring period were observed (Fig. 5). On the first monitoring day at Facility A, the secondary combustion chamber outlet temperature (A1 outlet) dropped to 800 ℃ at 10:00 and 837 ℃ at 11:00, which is below the 850 ℃ required by the “Standard for pollution control on the municipal solid waste incineration” (GB 18485-2014). This indicates that the combustion efficiency in the secondary combustion chamber of Facility A was poor; it was unable to maintain a stable temperature above 850 ℃ during certain periods, even when the gasifier was producing sufficient combustible gas. However, on the second day, the secondary combustion chamber inlet temperature (A2 inlet) was generally too high, reaching a maximum of 1,073 ℃, resulting in an excessively rapid waste gasification rate. Consequently, the organic matter was not fully oxidized and decomposed, as evidenced by the second day’s slag heat loss rate of 3.27%. The overall operational stability of Facility A’s secondary combustion chamber was suboptimal. Facility B, on the other hand, was able to maintain the secondary combustion chamber temperature consistently above 850 ℃

without any instances of excessive temperatures, with all readings remaining below 1,000 ℃, indicating that Facility B's combustion conditions were both favourable and stable.



Note: The threshold value is from GB 18485-2014.

Fig. 5. Secondary combustion chamber inlet and outlet temperature

2.2.3 Flue gas purification system

There are also several differences between the flue gas treatment systems at the two facilities, the most significant of which lies in the dust removal processes.

Facility A employs an electrostatic precipitator for dust removal, which captures the fly ash generated. At Facility B, wet electrostatic precipitation technology is used in the final stage of the flue gas purification process; the captured fly ash falls into a recirculating water tank beneath the equipment, where it is temporarily stored as sludge. It is subsequently returned to the gasifier in batches via sewage pumps, along with various wastewaters and leachate from waste, for disposal.

2.3 Pollutant emission comparison

2.3.1 Comparison of conventional pollutant emissions in flue gas

Removing acidic pollutants (HCl and SO_2) is an important stage in the cleaning of waste incineration flue gas and is also required for emission control (Dal Pozzo et al. 2018). Both facilities showed good control over SO_2 in the flue gas, with SO_2 concentrations in the three-day flue gas samples not exceeding 10 mg/Nm^3 (Fig. 6), far below the GB 18485-2014 requirement (100 mg/Nm^3). This is also due to the relatively low sulfur content in the waste. Among them, the

concentration in Facility A was lower, with no detection in samples A2 and A3 (<3 mg/Nm^3), while the lowest concentration in Facility B was 5.5 mg/Nm^3 in sample B3. Additionally, the S content in the waste fed into Facility A was slightly higher than that in Facility B, indicating that Facility A achieved better SO_2 control.

Since neither facility has a denitrification stage in their technical processes, the NO_x concentration in the flue gas emissions is relatively high. Especially for Facility A, the higher calorific value of the waste entering the furnace results in a higher temperature in the secondary combustion chamber, making the thermal NO_x formation mechanism dominant (Fu et al. 2020). Consequently, during the monitoring process, the NO_x concentration in the flue gas samples exceeded the standard, with the highest concentration in A3 reaching 698 mg/Nm^3. The NO_x concentration in the B3 flue gas sample of Facility B was 261 mg/Nm^3, almost reaching the emission limit of 300 mg/Nm^3, posing a risk of exceeding the limit.

Regarding the control of HCl, Facility A performed relatively poorly, with a concentration of 52 mg/Nm^3 in the first day's sample, which is close to the HCl emission limit (60 mg/Nm^3). This may be due to the higher Cl content in the waste fed into Facility A. The Cl content in the waste fed into Facility B was inherently low, and the wet desulfurization process showed better HCl control performance, with a maximum concentration of only 9.45 mg/Nm^3.

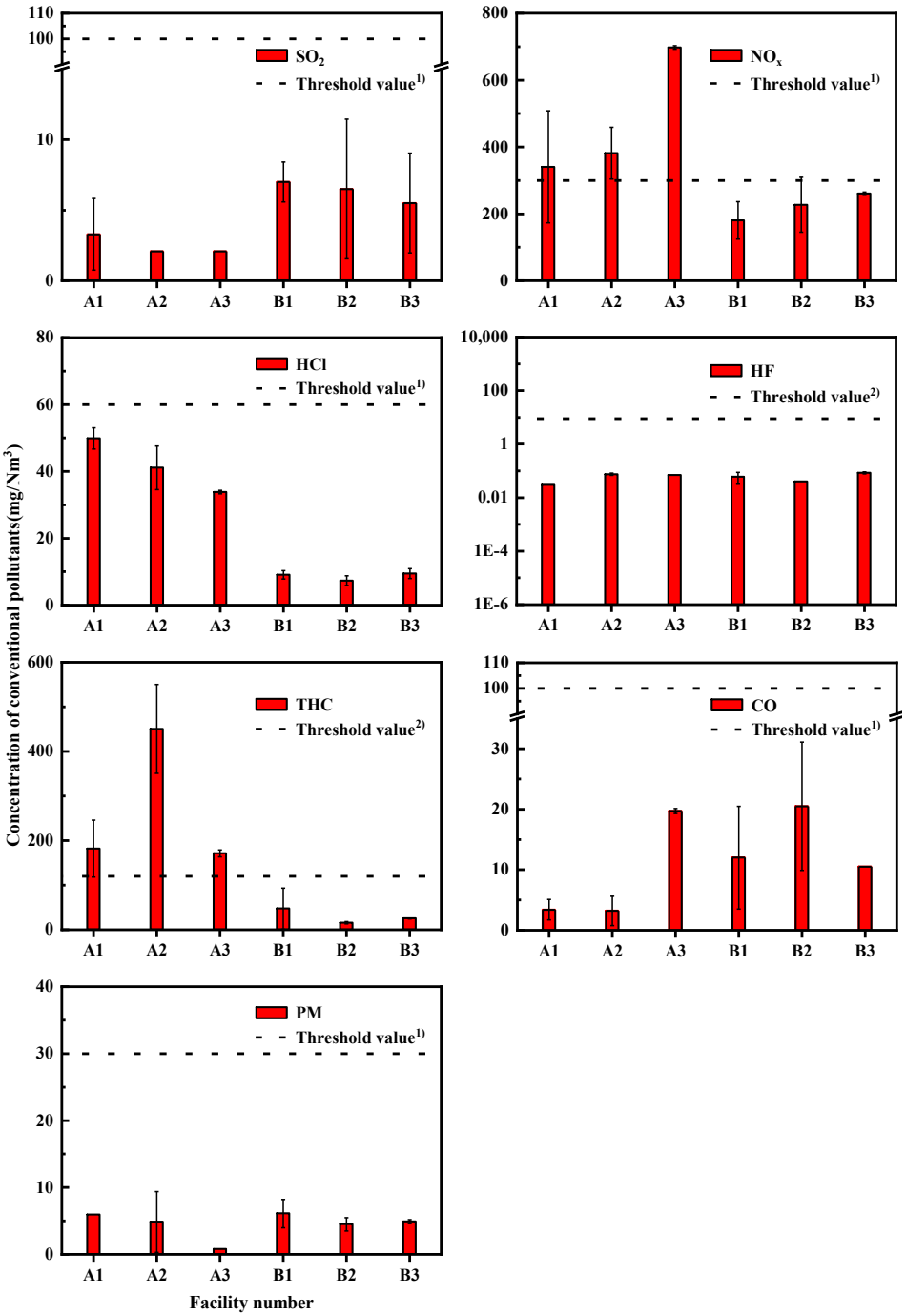
The concentration of HF in the flue gas of both A and B facilities did not reach 0.1 mg/Nm^3. The GB 16297-1996 "Integrated emission standard of air pollutants" limits HF emissions to below 9 mg/Nm^3, indicating that the overall corrosiveness of acidic gasses to the facilities is very low (Serris et al. 2009).

The THC concentration in the flue gas of Facility A exceeded the limit quite significantly. The emission limit set by GB 16297-1996 is 120 mg/Nm^3, while Facility A reached a maximum of 521 mg/Nm^3. THC mainly consists of incompletely oxidized volatile organic compounds, which may not be fully decomposed or burned during incineration due to factors such as uneven temperature and oxygen distribution. The THC concentration in Facility B was at a relatively low level with minimal fluctuations, with a minimum of only 15.7 mg/Nm^3.

The concentration and fluctuation range of CO were relatively smaller than those of THC, and both facilities met the requirement of less than 100 mg/Nm^3 in GB 18485-2014. The highest concentration was 20.5 mg/Nm^3 for the B2 sample. However, compared with the two facilities, Facility A had a higher content of highly volatile organic components such as plastics and rubber in its incoming municipal solid waste (Cabanes A 2020). These components may volatilize during the initial stage of combustion, forming high concentrations of THC. The combustion conditions in the secondary combustion chamber of Facility A were insufficient. There was a certain fluctuation in the CO concentration in the flue gas of Facility A, with a difference of 16.3 mg/Nm^3 between the A1 and A3 samples, which also proves that the operational stability of Facility A and the combustion conditions in the secondary combustion chamber were relatively poorer than those of Facility B.

Facility A employed a two-stage dust removal process, and the results showed that half of the PM concentrations in

the samples from Facility A were not detected (<0.9 mg/Nm^3). However, there were fluctuations in the emission concentrations. For example, the PM concentration in the first sample of the A1 flue gas was 11.33 mg/Nm^3, while the second sample was not detected. In the A2 flue gas, the first sample also showed detectable PM, while in the A3 samples, PM was not detected. Despite some fluctuations, the facility still fully met the standard requirements (30 mg/Nm^3). Facility B used a wet electrostatic precipitator to capture PM, and the removal effect on PM was also quite significant and stable, with an average concentration of only 5.4 mg/Nm^3, and no fluctuations were observed.



Notes: 1) is from GB18485-2014; 2) is from GB 16297-1996.

Fig. 6. Concentration of conventional pollutants in flue gas

2.3.2 Comparison of heavy metal emissions in flue gas

The concentrations of 15 heavy metals (Mn, As, Pb, Cr, Cd, Cu, Ni, Zn, Sb, Be, Sn, Co, V, Tl, Hg) in the flue gas were measured (Fig. 7). Facility A exhibited high Zn emissions in its flue gas, reaching a maximum of 449 μg/Nm^3. As mentioned above, the concentration of Zn in the waste fed into the furnace was relatively high compared with other metallic elements. Furthermore, the high Cl content in the waste reacts with heavy metals to form fine-particle metal chlorides with low boiling points, thereby accelerating the migration of heavy metals into the flue gas. When the temperature rises to 1,200 ℃, the volatilization rate of Zn can reach as high as 95% (Nowak et al. 2012), suggesting that a significant amount of $ZnCl_2$ may have formed in the flue gas, resulting in a higher proportion of Zn in the flue gas. The average concentration of Mn was 22.2 μg/Nm^3, second only to Zn. However, the concentration of Zn was 20 times that of Mn, while the Mn content in the waste was lower than that of Zn. Although the Zn content in the slag and fly ash from Facility A was also relatively high, this indicates to some extent that the process has a poor immobilization effect on Zn. The average concentrations of highly toxic heavy metals such as Sn, As, Tl and Be were all below 1 μg/Nm^3.

On the first monitoring day at Facility B, the concentration of Tl in the flue gas was high, at 83.6 μg/Nm^3 in the B1 flue gas; but the concentration dropped rapidly over the following two days to 17 and 0.3 μg/Nm^3, respectively. As the Tl content in the waste fed into Facility B on the second day was only 0.014 mg/kg, it is considered that the waste fed on the first day contained a relatively high proportion of Tl-containing electronic waste (Willner et al. 2021). Given the extreme toxicity of Tl (Lopes et al. 2018), particular attention must be paid to fluctuations in the composition of the waste fed into the furnace. Unlike Facility A, the maximum concentration of Zn in the flue gas at Facility B was only 39.6 μg/Nm^3, with even lower levels in the samples from the following two days, at 9.9 and 5.9 μg/Nm^3, respectively. Although Zn was the most abundant heavy metal in the waste fed into Facility B, its concentration was lower than that in the waste fed into Facility A. Furthermore, the concentrations of highly toxic heavy metals such as Hg, Pb, Cd and Be were all below 3 μg/Nm^3.

According to GB 18485-2014, the sum of Sb, As, Pb, Cr, Co, Cu, Mn and Ni must be below 1,000 μg/Nm^3, and the sum of Cd and Tl must be below 100 μg/Nm^3. As the heavy metal content in the waste fed into the furnace is not high, it can be seen from the figure that both Facility A and Facility B fully meet the emission limit requirements. The combined concentration of Sb+As+Pb+Cr+Co+Cu+Mn+Ni in the flue gas from Facility A was 38.6 μg/Nm^3, and that of Cd+Tl was 1.97 μg/Nm^3; for Facility B, these figures were 69.9 and 33.9 μg/Nm^3, respectively. Furthermore, the concentration of Hg in all flue gas samples was also extremely low.

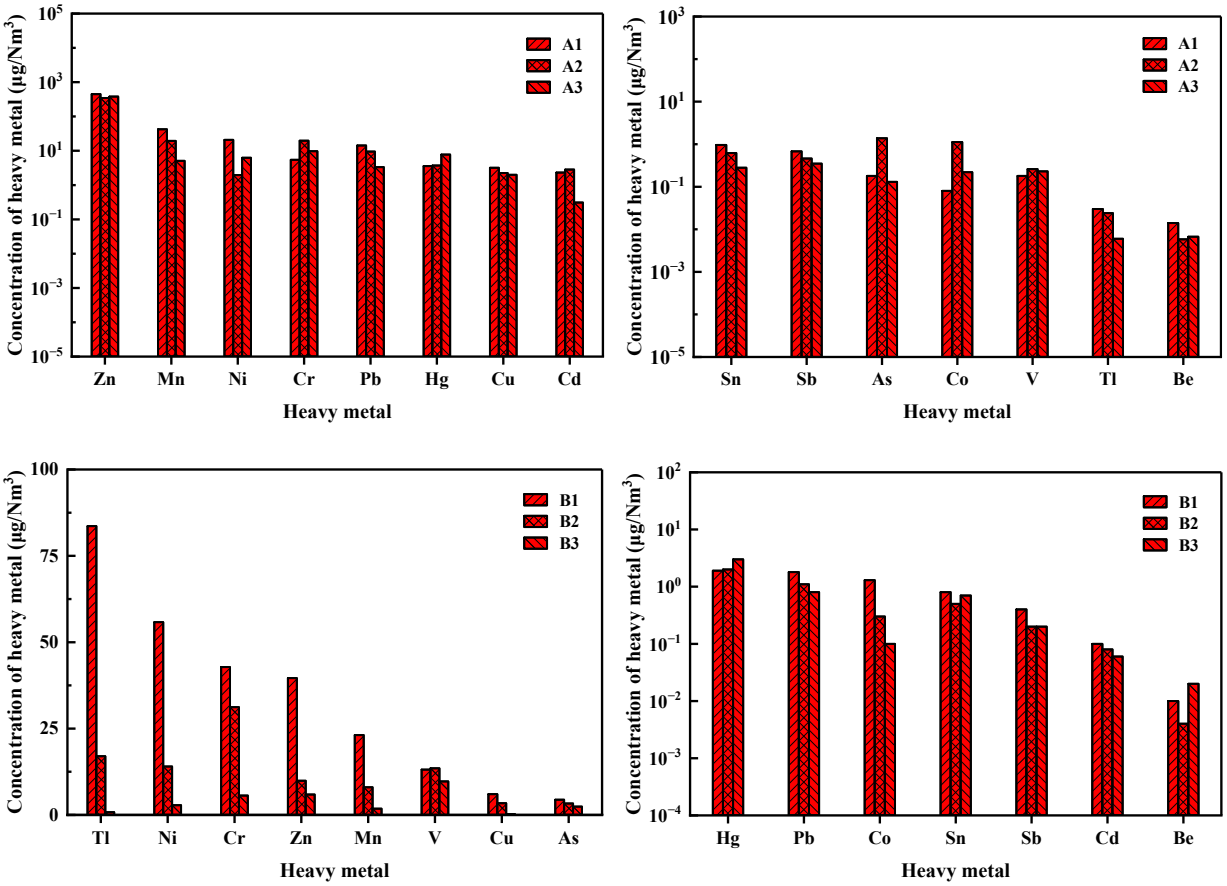


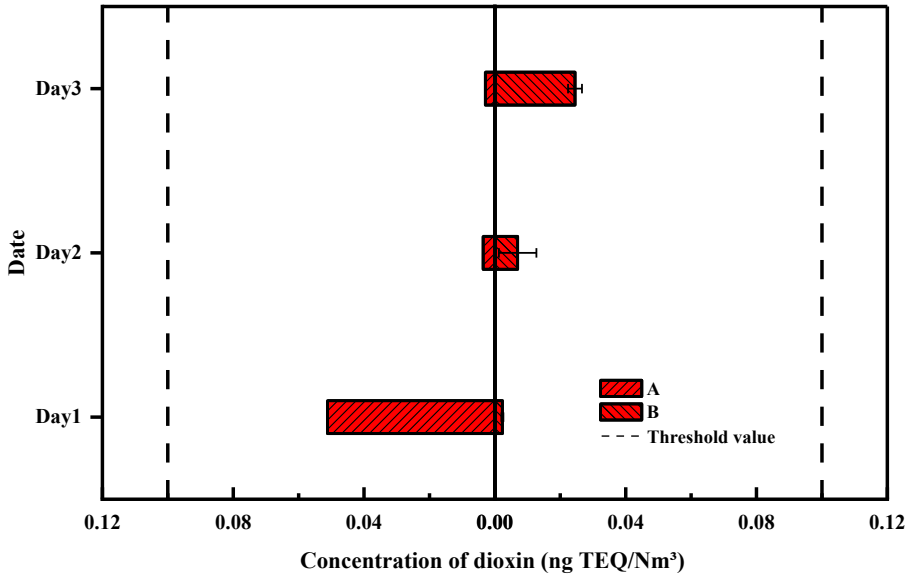
Fig. 7. Concentration of heavy metals in flue gas

2.3.3 Comparison of dioxin emissions in flue gas and fingerprint characteristics of homologues

Dioxin emissions in flue gas have always been a key concern in municipal solid waste heat treatment technology, and this is particularly true for small-scale facilities. Given the extreme toxicity of dioxins, their release poses a significant environmental risk in heat treatment facilities (Pham et al. 2019).

The two facilities demonstrated good performance in terms of dioxin pollution control, with emission concentrations both below the 0.1 ng TEQ/m^3 limit specified in GB 18485-2014 (Fig. 8). One reason for the low emissions is the low concentration of the heavy metals Cu and Ni in the flue gas, which act as catalysts for dioxin formation (Yan et al. 2009). The concentrations of Cu and Ni in the flue gas at Facility A were 2.47 and 9.67 μg/Nm^3, respectively, while at Facility B they were 3.2 and 24.2 μg/Nm^3, respectively. However, the dioxin concentration in the flue gas sample from Facility A on the first day was 0.0512 ng TEQ/m^3, while the average concentration over the following two days was only 0.0033 ng TEQ/m^3. This significant fluctuation was due to changes in the chlorine content of the waste; on the first day, the chlorine content of the waste entering the furnace was as high as 6,693 mg/kg, several times higher than on the subsequent two days. Furthermore, during the monitoring on the first day, the furnace temperature was relatively low; at low temperatures (<850 ℃), dioxins are highly prone to formation via de novo synthesis mechanisms (Wang et al. 2024). These two circumstances are likely the main reasons why the dioxin concentration in the flue gas sample on the first day was

significantly higher than that on the following two days. The maximum dioxin concentration in the flue gas from Facility B was only 0.0245 ng TEQ/m^3. However, it is evident that the emission concentration showed an upward trend over time, which may be due to changes in the chlorine content of the waste (Strezov et al. 2024), thereby altering the release of dioxins.



Note: The threshold value is from GB 18485-2014.

Fig. 8. Concentration of dioxin in flue gas

Based on the concentration distribution of dioxin congeners in the flue gas, it can be seen that the distribution characteristics of dioxin congeners in the flue gas from Facilities A and B are similar (Fig. 9); overall, polychlorinated dibenzofurans (PCDFs) account for a larger proportion. In Facility A's flue gas, the PCDFs comprised the pentachlorinated compounds 2,3,4,7,8-PeCDF (0.048 ng/Nm^3) and 1,2,3,7,8-PeCDF (0.028 ng/Nm^3), as well as the hexachlorinated compounds 1,2,3,6,7,8-HxCDF (0.028 ng/Nm^3) and 1,2,3,4,7,8-HxCDF (0.025 ng/Nm^3). Among these, 2,3,4,7,8-PeCDF accounted for the highest proportion at 17.84%. Furthermore, the concentrations of the tetrachlorinated compound 2,3,7,8-TCDF and the heptachlorinated compound 1,2,3,4,6,7,8-HpCDF were also high, at 0.035 and 0.03 ng/Nm^3, respectively, second only to 2,3,4,7,8-PeCDF. The highest mass concentration among the PCDDs was that of OCDD, at 0.012 ng/Nm^3, but this accounted for only 4.46% of the total.

Unlike Facility A, at Facility B, hexachlorinated and heptachlorinated compounds accounted for the largest proportion of PCDF congeners, with 1,2,3,4,6,7,8-HpCDF having the highest concentration among all congeners, reaching 0.0159 ng/Nm^3 and accounting for 16.37%. This was followed by the octachlorinated compound OCDF, with a mass concentration of 0.0124 ng/Nm^3, accounting for 12.77%. In contrast, the mass concentration of 2,3,4,7,8-PeCDF at Facility B was relatively low at 0.048 ng/Nm^3, accounting for 9.90% of the total concentration of isomers. As with Facility A, the highest concentration among the PCDD congeners in Facility B was also OCDD (0.012 ng/Nm^3), accounting for 9.21%. The above results indicate that the distribution characteristics of dioxin congener concentrations differ slightly

even among furnaces of the same type, which may be attributed to differences in technical processes and the physical composition of the waste.

The PCDDs/PCDFs ratio indicates the formation mechanism of dioxins (Tuppurainen et al. 1998); a value of PCDDs/PCDFs<1 indicates that dioxins are primarily generated via de novo synthesis, while a value of PCDDs/PCDFs>1 indicates that dioxins are primarily generated via precursor reactions (Li et al. 2023). The PCDDs/PCDFs results for the flue gas from both gasification incinerators were 0.2, indicating that the PCDDs/PCDFs in the flue gas were primarily formed via de novo synthesis. This is likely primarily due to the cooling process in the post-combustion zone (250-400 ℃), where HCl (Cl^-), O_2 and H_2O in the flue gas undergo heterogeneous catalytic reactions on the surface of carbon-containing fly ash, resulting in the formation of small amounts of dioxin pollutants (Zhou et al. 2006).

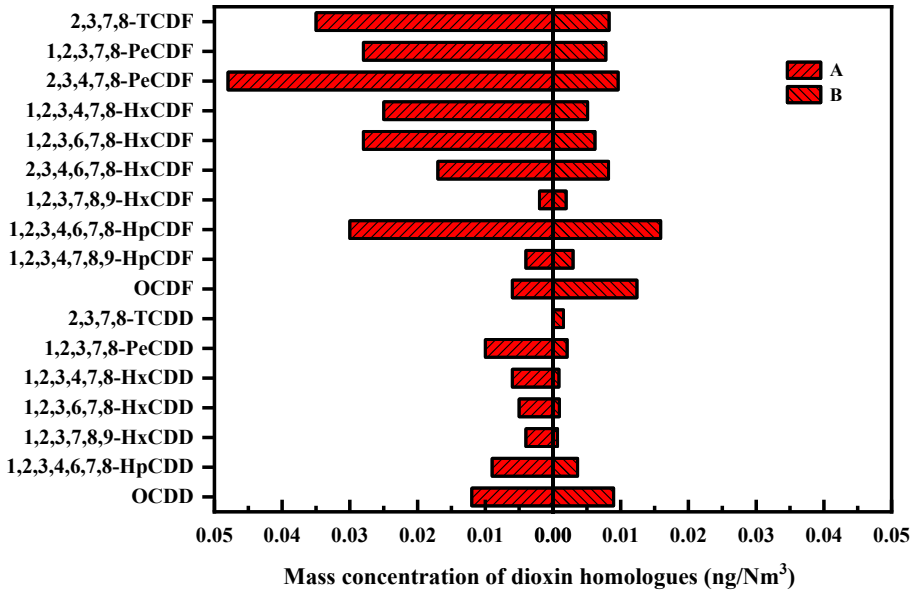


Fig. 9. Mass concentration of dioxin congeners in flue gas

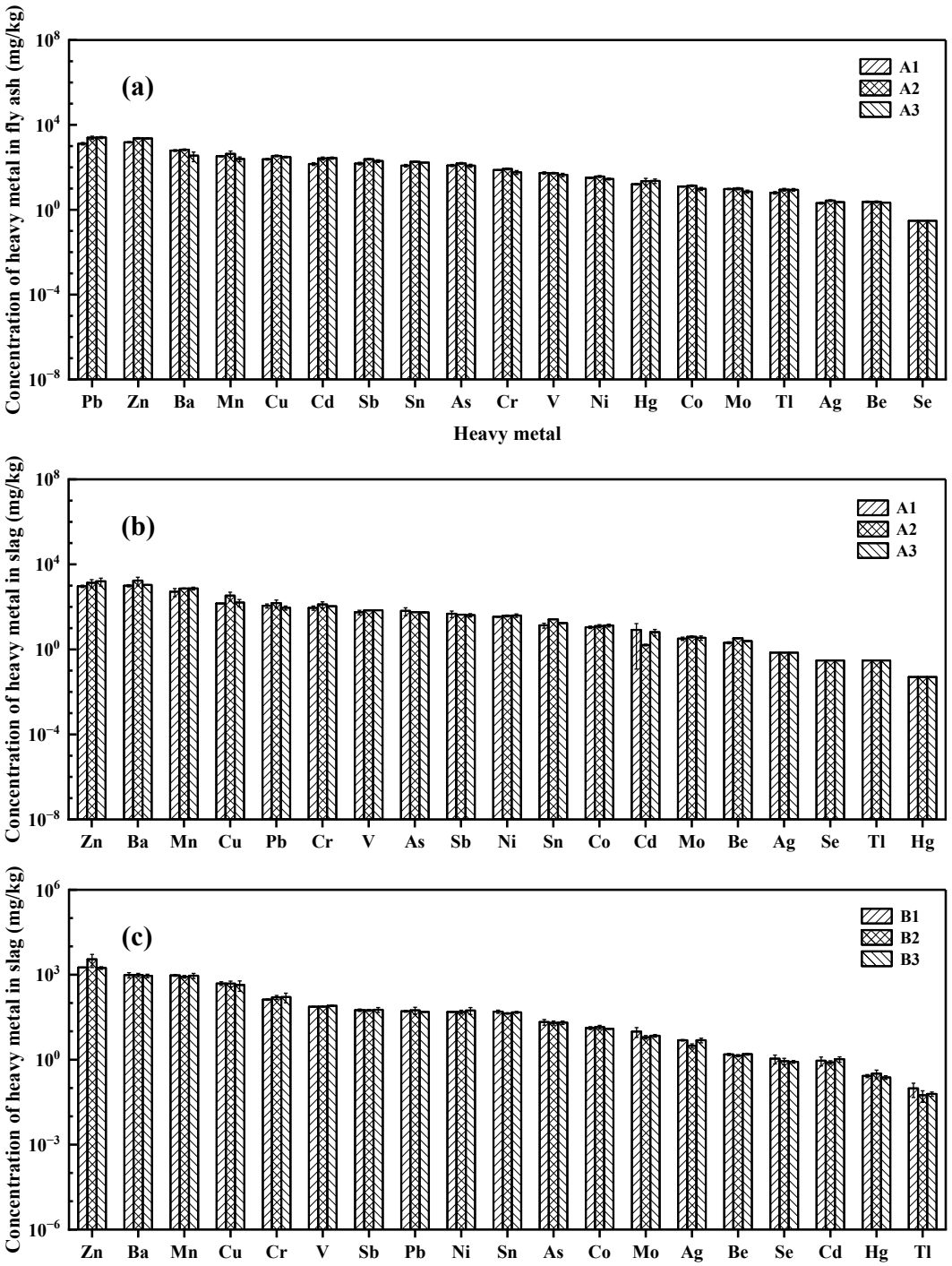
2.3.4 Comparison of heavy metal emissions in fly ash and slag

As fly ash from Facility B could not be collected, this section considers only the heavy metal content in the fly ash from Facility A.

The results indicate that the concentrations of Zn, Ba and Mn are generally high in both the bottom ash and the fly ash. Furthermore, the highest concentration of Pb in the fly ash from Facility A reached 2,543.3 mg/kg, whereas the highest concentration in the bottom ash was 151 mg/kg (Fig. 10a and b). The addition of Cl and S during the treatment process promotes greater migration of Pb into fly ash (Hu et al. 2018). The high Cl content in the waste fed into Facility A's furnace is likely the primary cause of this phenomenon. Due to the high Ba content in the waste fed into Facility A's furnace, the concentration of Ba in the slag from Facility A is relatively high, reaching 1,725 mg/kg, with the majority of Ba ultimately being immobilized in the slag.

For Facility B, similar to Facility A, the concentrations of Zn, Ba and Mn in the slag were relatively highest. As Zn

was the most abundant heavy metal element in the waste fed into the furnace, its concentration in the slag was also higher than that of other elements, at 2,348 mg/kg (Fig. 10c). Furthermore, the aforementioned low concentration of Zn in the flue gas demonstrates that Facility B achieves better immobilization of Zn compared with Facility A. The concentrations of the remaining heavy metal elements were all below 1,000 mg/kg, indicating that the slag is relatively safe. Overall, the proportions of various heavy metals in the slag from Facilities A and B were also quite similar.



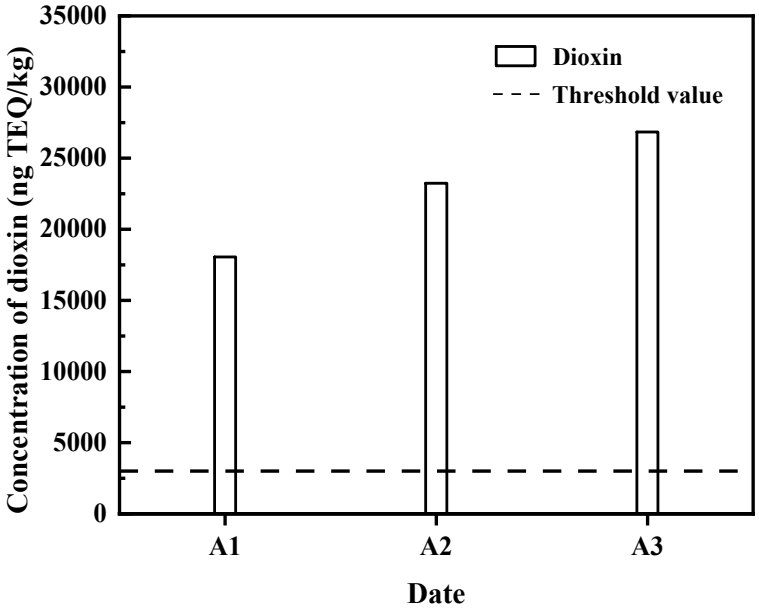
Note: When the content is below the detection limit, it is plotted as half the detection limit.

Fig. 10. (a) Concentration of heavy metals in fly ash from Facility A, (b) Concentration of heavy metals in slag from Facility A, (c) Concentration of heavy metals in slag from Facility B.

2.3.5 Comparison of dioxin emissions in fly ash and slag and fingerprint characteristics of homologues

As Facility B does not produce fly ash, this section considers only the dioxin emission levels and the distribution of their congeners in the fly ash from Facility A.

In contrast to the levels of dioxins in flue gas, the concentrations of dioxins in fly ash samples from Facility A were all above 15,000 ng TEQ/kg (Fig. 11), with the highest reaching 26,833 ng TEQ/kg. This exceeds the limit of 50 ng TEQ/kg more than 500 times the limit specified in the "Technical specification for pollution control of fly ash from municipal solid waste incineration" (HJ 1134-2020), which stipulates that the total dioxin residue in fly ash intended for resource recovery must not exceed 50 ng TEQ/kg and nearly nine times the requirement of the "Standard for pollution control on the landfill site of municipal solid waste" (GB 16889-2024), which specifies that dioxin levels in fly ash entering landfills must be below 3,000 ng TEQ/kg. This indicates that the majority of dioxins in flue gas have migrated and ultimately accumulated in fly ash; it also suggests that the fly ash generated by the facility poses an environmental risk and should be treated to meet relevant standards before being recycled or landfilled. The role of Cl remains dominant, and the concentration of the heavy metal Cu in the fly ash was 297 mg/kg, which is relatively high compared with other heavy metal elements. The high Cl content in the waste and the Cu in the fly ash form copper chlorides (such as $CuCl_2$ and CuCl), and copper chlorides are considered the most potent metal catalysts for dioxin formation (Zhang et al. 2019). Furthermore, it can be observed that the dioxin content in the fly ash exhibited an upward trend over time, which is the exact opposite of the trend in the flue gas. This indicates that the release of dioxins from Facility A has essentially reached a dynamic equilibrium between the flue gas and the fly ash.



Note: The threshold value is from GB 16889-2024.

Fig. 11. Concentration of dioxin in fly ash of Facility A

The distribution of dioxin congeners in fly ash shows that it is generally similar to that in flue gas, with

tetrachlorinated and pentachlorinated compounds again dominating. Furthermore, 2,3,4,7,8-PeCDF was the most abundant congener, with a mass concentration and proportion of 29,886 ng/kg and 20.31% respectively (Fig. 12); this characteristic is consistent with that observed in large-scale municipal waste incineration facilities (Liu et al. 2013). This was followed by 1,2,3,4,7,8-HxCDF (15,140 ng/kg), which is nearly half that of 2,3,4,7,8-PeCDF. At the same time, due to its toxicity equivalence factor (TEF = 1), 2,3,4,7,8-PeCDF also contributes the highest toxicity equivalence among all congeners and is the congener that contributes most to the total TEQ. It can be seen that, whether for the control of dioxin pollutants in flue gas or fly ash, limiting the formation of 2,3,4,7,8-PeCDF is crucial. The congener with the lowest concentration in both flue gas and fly ash was 2,3,7,8-TCDD, with a concentration of 983 ng/kg in fly ash. The PCDDs/PCDFs ratio in fly ash was 0.251, which was very close to the result in flue gas, indicating that the dioxin formation mechanism in fly ash was also de novo synthesis. This further proves that the dioxins in fly ash mainly originate from the adsorption and deposition of flue gas, rather than significant secondary synthesis occurring in the fly ash itself.

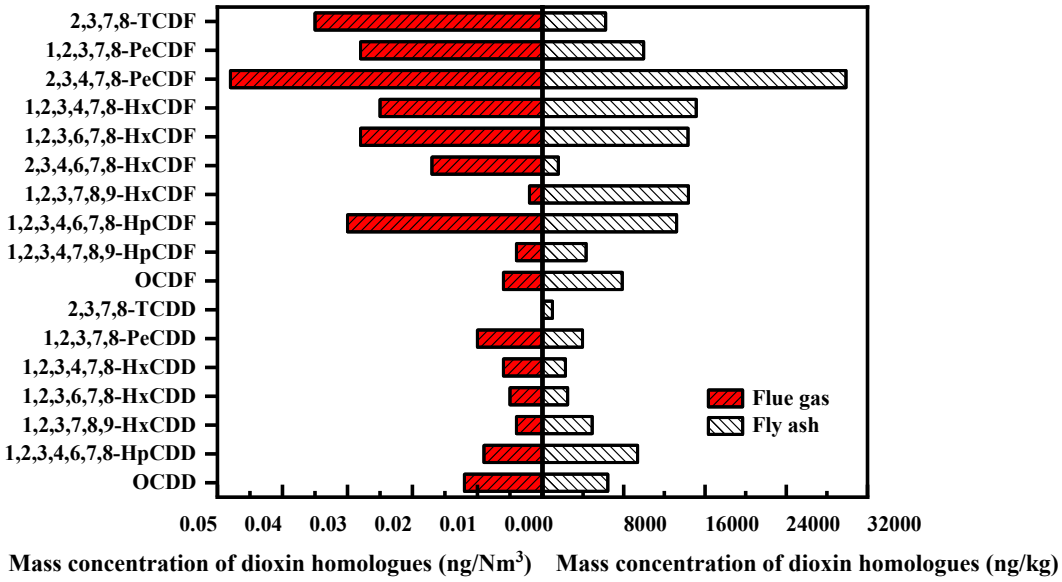


Fig. 12. Mass concentration of dioxin congeners in the flue gas and fly ash of Facility A

2.4 HSC thermodynamic equilibrium simulation NOx and incompletely combusted gases

2.4.1 Thermodynamic equilibrium model and parameter input

1. Thermodynamic equilibrium model

The equilibrium reaction model used in the thermodynamic equilibrium simulations in this study is based on a constant-pressure system (Fig. 13).

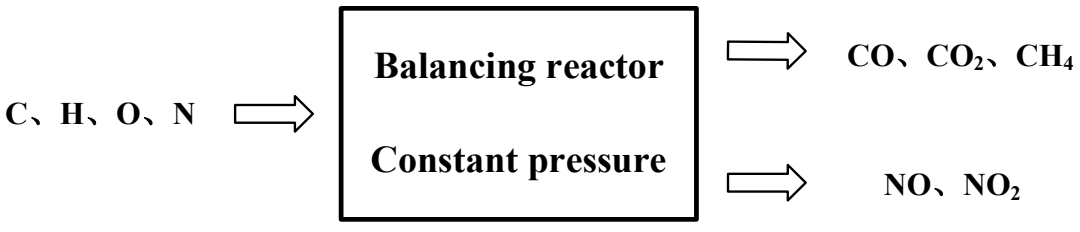


Fig. 13. Thermodynamic equilibrium calculation model

2. Simulate initial parameters and element inputs

The temperature (T), pressure (P) and air excess coefficient (λ) in the reactor were set at 400 - 900 ℃, 1.0 bar and 0.3, respectively. The thermodynamic simulation calculations used the following input parameters: 1 kg of the molar quantities of C, H, O and N in the municipal solid waste feedstock for each facility, as well as the theoretical requirements for O_2 and N_2 in the different atmospheres used for heat treatment at each facility (Table 6).

Table 6. Simulated input elements and values

Facilities	The amounts of each element substance in the input domestic waste(kmol)				Theoretical oxygen requirement (kmol)	Theoretical nitrogen requirement (kmol)
	C	H	O	N		
A	4.24×10^{-2}	8.04×10^{-2}	9.63×10^{-3}	10.0×10^{-4}	3.37×10^{-2}	1.27×10^{-1}
B	3.16×10^{-2}	6.45×10^{-2}	1.50×10^{-2}	4.28×10^{-4}	2.35×10^{-2}	8.85×10^{-2}

2.4.2 Thermodynamic equilibrium simulation of NOx

In the HSC simulations, NO_x was assumed to consist primarily of NO and NO_2. The simulated trends for NO and NO_2 were broadly similar across both facilities, with NO increasing whilst NO_2 remained largely unchanged. This is because NO_2 is unstable at high temperatures and decomposes into NO and O_2. Consequently, the equilibrium concentration of NO_2 is strongly suppressed. The HSC simulation results indicate that under oxygen-deficient conditions, the equilibrium concentrations of NO and NO_2 are extremely low (Fig. 14a and b), suggesting that the primary combustion chamber itself generates virtually no NO_x. The measured flue gas NO_x concentrations at each facility (A: 473 mg/m^3, B: 223 mg/m^3) were significantly higher than the simulated values for the primary combustion chamber, confirming that NO_x primarily originates from the oxygen-enriched combustion of high-temperature flue gas in the secondary combustion chamber. At Facility A, fluctuations in secondary combustion chamber temperature led to intense thermal NO_x formation, resulting in exceedances of emission limits. Facility B has a relatively stable secondary combustion chamber temperature, with NO_x levels close to the limit. This comparison reveals a strong correlation between NO_x formation and the operating conditions of the secondary combustion chamber, providing a basis for a unified interpretation of the simulation results and the measured flue gas data.

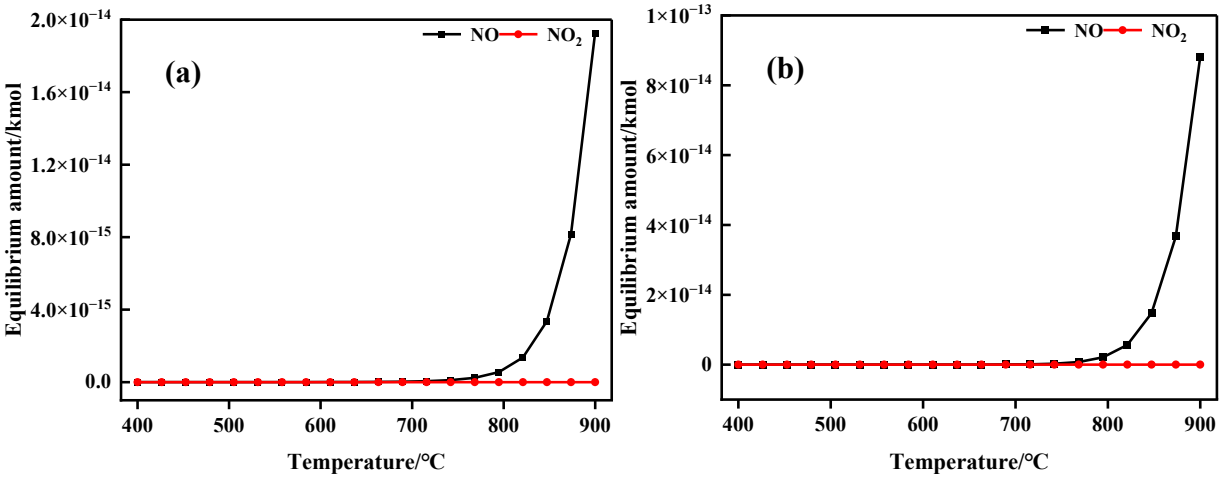


Fig. 14. (a) Simulation results of NO and NO_2 equilibrium composition from Facility A, (b) Simulation results of NO and NO_2 equilibrium composition from Facility B.

2.4.3 Thermodynamic equilibrium simulation of incompletely combusted gases

In the HSC simulation, the gases resulting from incomplete combustion were assumed to consist primarily of CO and CH_4; the results revealed the distribution patterns of products within the temperature range of the primary combustion chamber for different processes. The simulation results for the two facilities indicate that the trends in CO, CO_2, and CH_4 with respect to temperature are quite similar (Fig. 15a and b). The fundamental reason is that they all exist in an oxygen-deficient, reducing atmosphere, and the conversion of carbon is governed by the same thermodynamic equilibrium. Specifically, CO increases with rising temperature due to endothermic reactions (the Boudouard reaction: $C + CO_2 \rightleftharpoons 2CO$, and the water-gas reaction: $C + H_2O \rightleftharpoons CO + H_2$), while CO_2 decreases as it is consumed and decomposed. CH_4 is produced in large quantities in the low-temperature zone of the primary combustion chamber but is virtually absent at high temperatures. Although there are slight differences in process and waste composition, the thermodynamically dominant reactions are identical, resulting in consistent qualitative trends. From a thermodynamic perspective, this commonality validates the universality of carbon conversion patterns under anoxic/anaerobic conditions. It also provides a theoretical basis for explaining variations in THC emissions across different facilities. In practice, significant fluctuations and exceedances of THC levels were observed in the flue gas from Facility A, demonstrating that operational fluctuations in Facility A's secondary combustion chamber were the primary cause of this phenomenon. The simulation results confirm the fundamental influence of process differences and actual facility operating conditions on pollutant formation pathways.

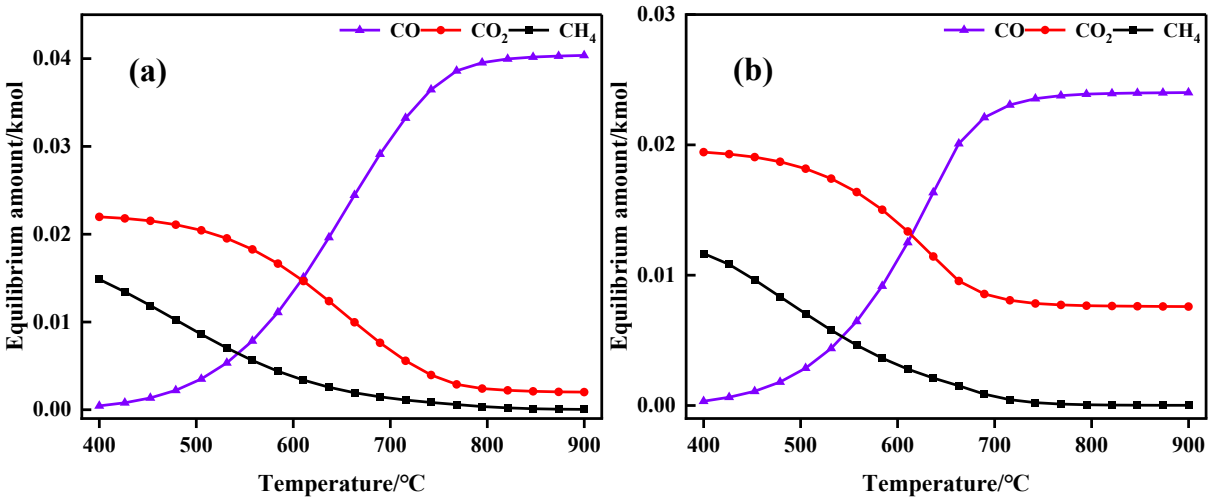


Fig. 15. (a) Simulated results of the CO, CO_2, and CH_4 equilibrium composition from Facility A, (b) Simulated results of the CO, CO_2, and CH_4 equilibrium composition from Facility B.

3 Conclusions

Monitoring was carried out on two small-scale gasification incinerators located in different regions. The results revealed that, during operation, the secondary combustion chamber at Facility A experienced periods when the temperature fell below 850 ℃, while the secondary combustion chamber at Facility B operated stably. In terms of environmental risk, the maximum concentrations of NO_x and THC among the conventional pollutants in Facility A's flue gas reached 698 and 521 mg/Nm^3, respectively, exceeding the requirements of GB 18485-2014. Furthermore, significant fluctuations were observed during the monitoring period, which further confirms the unstable operation of this facility and the poor combustion efficiency of its secondary combustion chamber. Concentrations of heavy metal pollutants in Facility A's flue gas were also relatively higher than those in Facility B; the concentration of Zn reached a maximum of 449 μg/Nm^3, while the average concentration of Mn was 22.2 μg/Nm^3, second only to Zn, demonstrating that the process is less effective at immobilizing Zn. In contrast to Facility A, the maximum concentration of Zn in the flue gas from Facility B was only 39.6 μg/Nm^3, and was even lower in the samples from the latter two days. It is worth noting that the concentration of Tl in the flue gas on the first monitoring day was 83.6 μg/Nm^3, but fell rapidly over the following two days, indicating that Facility B has a relatively better immobilization effect on heavy metal pollutants. The levels of dioxin emissions in the flue gas from both facilities were low, with concentrations ranging from 0.023 to 0.0512 ng TEQ/m^3. The distribution characteristics of dioxin congeners in the flue gas from both facilities were broadly similar. In Facility A, 2,3,4,7,8-PeCDF accounted for the highest proportion (17.84%) of all dioxin congeners in the flue gas, while in Facility B, 1,2,3,4,6,7,8-HpCDF accounted for the highest proportion (16.37%) of all congeners. The PCDDs/PCDFs ratio indicates that the primary synthesis pathway for PCDDs/PCDFs in the flue gas from both facilities is de novo synthesis. The concentrations of Zn, Ba and Mn were generally high in both the slag and the fly ash from Facility A. Furthermore,

the highest concentration of Pb in the fly ash from Facility A reached 2,543.3 mg/kg, while the highest concentration in the slag was 151 mg/kg. The Zn concentration in the slag from Facility B was 2,348 mg/kg, with the concentrations of all other heavy metal elements below 1,000 mg/kg, indicating that the slag is relatively safe. Overall, the proportions of various heavy metals in the slag from Facilities A and B were relatively similar. Dioxin pollutants exhibited an accumulation effect in the fly ash from Facility A, with the highest concentration reaching 26,833 ng TEQ/kg, far exceeding regulatory standards; the environmental risk posed by the fly ash is significant. Among the fly ash, 2,3,4,7,8-PeCDF was the most prevalent congener (20.31%). Finally, thermodynamic equilibrium calculations for NO_x and incomplete combustion gases in the flue gas were performed using HSC Chemistry software. Comparison with measured values revealed that the simulated equilibrium concentrations of NO and NO_2 were extremely low, confirming that NO_x primarily originates from oxygen-enriched combustion in the high-temperature flue gas of the secondary combustion chamber. CH_4 is generated in large quantities in the low-temperature zone of the primary combustion chamber, but is virtually absent at high temperatures. The above findings confirm that the operating conditions of the secondary combustion chamber are strongly correlated with the generation of NO_x and unburned gases.

Overall, Facility A exhibits relatively poor operational stability, with both NO_x and THC levels exceeding regulatory limits. In contrast, Facility B has lower emission levels for all pollutants, presents a relatively lower environmental risk, and demonstrates high operational stability, making it a technical benchmark for facilities of this type. This also highlights regional variations in the fundamental properties of municipal solid waste and the heat treatment processes and outcomes.

References

Arista N.I.D, Handayani D, Ernawati N (2023) Is It Possible to Implement the Same Circular-Economy Concept in Rural and Urban Areas? Study on Willingness to Pay for Household Waste. Sustainability 15: 5843. https://doi.org/10.3390/su15075843

Cabanes A, Valdés FJ, Fullana A (2020) A review on VOCs from recycled plastics. Sustain Mater Technol 25: e00179. https://doi.org/10.1016/j.susmat.2020.e00179

Cheng J, Chang S, Gong Y, Li W, Zhu X, Li D (2025) Simulation Study on the Process Flow of High-Temperature Gasification of Solid Waste and Household Waste for Hydrogen Production. Adv Environ Prot 15: 224-238. https://doi.org/10.12677/aep.2025.152029

Dal Pozzo, A, Guglielmi D, Antonioni G, Tugnoli A (2018) Environmental and economic performance assessment of alternative acid gas removal technologies for waste-to-energy plants. Sustain Prod Consum 16: 202-215. https://doi.org/10.1016/j.spc.2018.08.004

Du Y, Ju T, Meng Y, Lan T, Han S, Jiang J (2021) A review on municipal solid waste pyrolysis of different composition for gas production. Fuel Process Technol 224: 107026. https://doi.org/10.1016/j.fuproc.2021.107026

Fu Z, Gao H, Zeng Z, Liu J, Zhu Q (2020) Generation characteristics of thermal NO_x in a double-swirler annular combustor under various inlet conditions. Energy 200: 117487. https://doi.org/10.1016/j.energy.2020.117487

Hu J, Wang S, Xu H, Wu T (2018) Partitioning of Pb during Municipal Solid Waste Incineration. J East China Univ Sci Technol (Nat Sci Ed) 44: 800-806. https://doi.org/10.14135/j.cnki.1006-3080.20171030003

Jeon MK, Shin JM, Park JJ, Park GI (2012) Simulation of Cs behavior during the high temperature voloxidation process

using the HSC chemistry code. J Nucl Mater 430: 37-43. https://doi.org/10.1016/j.jnucmat.2012.06.040

Jia T, Chen S, Teng L, Zhang R, Yuan G, Chen Y, Yin L (2024) Characteristics and mechanism of slagging in a 500 t/d MSW incinerator. Journal of the Energy Institute 114: 101585. https://doi.org/10.1016/j.joei.2024.101585

Jia Y, Wang Z, Xia S, Li X, Xing F (2015) Source Analysis and Pollution Risk Assessment of Heavy Metals from Shanghai Domestic Waste. Environ Sanitat Eng 23: 31-34.

Kots PA, Vance BC, Quinn CM, Wang C, Vlachos DG (2023) A two-stage strategy for upcycling chlorine-contaminated plastic waste. Nat Sustain 6: 1258-1267. https://doi.org/10.1038/s41893-023-01147-z

Lan H (2010) Research Advance On Improvement Of Plastic Property By Barium sulfate. China Powder Industry. 7-9.

Lei M, Xie B, Hai J, Zhang J, Cheng T, Lu J (2019) Emission characteristics and inhalation exposure risk assessment of PCDD/Fs from small-scale domestic waste incinerator. Environ Pollut Control 41: 1471-1476. https://doi.org/10.15985/j.cnki.1001-3865.2019.12.016

Li C, Jiang Y, Shao, Y Gao, G Fan, M Zhang, L Zhang, S Xiang J, Hu S, Wang Y, Hu X (2024) Quantification of degree of interactions during co-pyrolysis of nine typical carbonaceous wastes. Renew Energy 227: 120569. https://doi.org/10.1016/j.renene.2024.120569

Li C, Liu G, Qin S, Zhu T, Song J, Xu W (2023) Emission reduction of PCDD/Fs by flue gas recirculation and activated carbon in the iron ore sintering. Environ Pollut 327: 121520. https://doi.org/10.1016/j.envpol.2023.121520

Li J, Yang X, Hou L, Yan B, Cheng Z, Zhao J, Chen G (2024) Pyrolysis-combustion of rural solid waste: Self-sustaining operation and pollutants emission. Fuel 368: 131575. https://doi.org/10.1016/j.fuel.2024.131575

Liu W, Tian Z, Li H, Xie H, Xiao K, Li C, Tang C, Zheng M (2013) Mono- to Octa-chlorinated PCDD/Fs in stack gas from typical waste incinerators and their implications on emission. Environ Sci Technol 47: 9774-9780. https://doi.org/10.1021/es402136s

Li X, Li L, Liu M, Li W, Cui C, Huang Q, Chen C, Yan D (2024) Emission characteristics of dioxin from small-scale high-temperature treatment facilities for rural waste in the Tibetan Plateau region. Front Environ Sci Eng 19: 21. https://doi.org/10.1007/s11783-025-1941-7

Lopes EJ, Queiroz N, Yamamoto CI, da Costa Neto PR (2018) Evaluating the emissions from the gasification processing of municipal solid waste followed by combustion. Waste Manage 73 :504-510. https://doi.org/10.1016/j.wasman.2017.12.019

Nowak B, Frías Rocha S, Aschenbrenner P, Rechberger H, Winter F (2012) Heavy metal removal from MSW fly ash by means of chlorination and thermal treatment: Influence of the chloride type. Chem Eng J 179: 178-185. https://doi.org/10.1016/j.cej.2011.10.077

Peng Y, Chen J, Lu S, Huang J, Zhang M, Buekens A, Li X, Yan J (2016) Chlorophenols in Municipal Solid Waste Incineration: A review. Chem Eng J 292: 398-414. https://doi.org/10.1016/j.cej.2016.01.102

Pham MTN, Anh HQ, Nghiem XT, Tu BM, Dao TN, Nguyen MH (2019) Characterization of PCDD/Fs and dioxin-like PCBs in flue gas from thermal industrial processes in Vietnam: A comprehensive investigation on emission profiles and levels. Chemosphere 225: 238-246. https://doi.org/10.1016/j.chemosphere.2019.03.024

Serris E, Cournil MM, Peultier J (2009) Modelling and Simulation of Acid Gas Condensation in an Industrial Chimney. Int J Chem React Eng 7: A39. https://doi.org/10.2202/1542-6580.1881

Strezov V, Zhou X, Evans T, Kan T, Taylor MP (2024) Investigation of the effect of chlorine in different additives on dioxin formation during high temperature processing of iron ore. Ecotoxicol Environ Saf 288: 117406. https://doi.org/10.1016/j.ecoenv.2024.117406

Teng H, Zhou K (2023) Designing a sustainable collection and transportation routes for domestic wastes in the agro-pastoral ecotone of the Tibetan Plateau. J Environ Manage 347: 119130. https://doi.org/10.1016/j.jenvman.2023.119130

Teng W, You Z, Liao Y, Chen Z, Qi X, Ma X (2024) Characteristics of heavy metal migration in the gasification-combustion process of rural solid waste: Influencing factors and mechanisms. Waste Manage 190: 350-359. https://doi.org/10.1016/j.wasman.2024.09.031

Tuppurainen K, Halonen I, Ruokojärvi P, Tarhanen J, Ruuskanen J (1998) Formation of PCDDs and PCDFs in municipal waste incineration and its inhibition mechanisms: A review. Chemosphere 36: 1493-1511. https://doi.org/10.1016/S0045-6535(97)10048-0

Turner A, Filella M (2020) The influence of additives on the fate of plastics in the marine environment, exemplified with barium sulphate. Mar Pollut Bull 158: 111352. https://doi.org/10.1016/j.marpolbul.2020.111352

Wang P, Xie F, Yan F, Jiao X, Shen X, Chen H, Lin H, Wu H, Zhang Z (2024) Formation, migration, and removal mechanisms of PCDD/Fs throughout the temperature range (850°C-150°C) in a full-scale MSW incinerator: The invention of novel high-temperature PCDD/F sampling device. Chem Eng J 500: 156660. https://doi.org/10.1016/j.cej.2024.156660

Wang Q (2023) Corrosion mechanism of refractories during high temperature melting of municipal solid waste incineration (MSWI) fly ash and recipe optimization. East China Norm Univ. https://doi.org/10.27149/d.cnki.ghdsu.2023.003794

Willner J, Fornalczyk A, Jablonska-Czapla M, Grygoyc K, Rachwal M (2021) Studies on the Content of Selected Technology Critical Elements (Germanium, Tellurium and Thallium) in Electronic Waste. Materials 14: 3722. https://doi.org/10.3390/ma14133722

Yan M, Li X, Zhang X, Liu K, Yan J, Cen K (2009) Mechanism of PCDD／Fs formation from PAHs catalyzed by metal compounds. CIESC Journal 60: 1254-1259.

Yang L, Liu G, Zhu Q, Zheng M (2019) Small-scale waste incinerators in rural China: Potential risks of dioxin and polychlorinated naphthalene emissions. Emerging Contam 5: 31-34. https://doi.org/10.1016/j.emcon.2019.01.001

Yang Z, Ni Y, Zhang Q, Chen J, Liang X (2004) Distribution characters of polychlorinated dibenzo-p-dioxins and dibenzofurans in fly ash or slag from municipal waste incineration. China Environ Sci 24: 524-527.

Yuan D, Xu M, Yan Z, Wang X, Wang J, Ge H, Zhao Y, Meng X (2025) Slagging characteristics of industrial waste incineration system in sections with different temperatures. J Energy Inst 120: 102107. https://doi.org/10.1016/j.joei.2025.102107

Zhang M, Li X, Chen T (2019) Copper chloride catalyzed PCDD/F-formation: Experiments and PCDD/F-signatures. Acta Sci Circumstantiae 39: 2735-2746. https://doi.org/10.13671/j.hjkxxb.2019.0062

Zhao B, Hu X, Lu J (2022) Analysis and discussion on formation and control of dioxins generated from municipal solid waste incineration process. J Air Waste Manag Assoc 72: 1063-1082. https://doi.org/10.1080/10962247.2022.2100843

Zhao D, Wu Q, Zeng Y, Zhang J, Mei A, Zhang X, Gao S, Wang H, Liu H, Zhang Y, Qi S, Jia X (2023) Contamination and human health risk assessment of heavy metal(loid)s in topsoil and groundwater around mining and dressing factories in Chifeng, North China. Int J Coal Sci Technol 10: 8. https://doi.org/10.1007/s40789-023-00568-7

Zhao J, Guo E, Wang Y, Kang Y, Wu J, Zhang Y, Zhang M (2026) Ecological drought patterns and drivers in Inner Mongolia using a modified temperature vegetation drought index. Ecosphere 17: e70600. https://doi.org/10.1002/ecs2.70600

Zhou L, Zhao Y (2006) De Novo Synthesis of Dioxins Formation. Industrial Furnace 28: 13-18.

Declarations

Ethics approval: This is not applicable.

Consent to participate: This is not applicable.

Consent for publication: This is not applicable.

Competing interests: The authors declare no competing interests.

Data Availability Statement: This is not applicable.

Acknowledgments: This work was supported by the National Key Research and Development Program of China (grant number 2024YFC3909005, 2024YFC3810303)

Funding: National Key Research and Development Program of China (grant number 2024YFC3909005, 2024YFC3810303)

Authors' Contributions: Zitong Liu, Chao chen, Li Li, Lei Wang, Dahai Yan contributed to the study conception and design. Material preparation, data collection and analysis were performed by Zitong Liu. The first draft of the manuscript was written by Zitong Liu. Chao chen, Li Li, Lei Wang, Dahai Yan commented on previous versions of the manuscript and also offered advice on the article writing and the drawing of the figures and tables. All authors read and approved the final manuscript.